Impact of the propagation model on the capacity in small-cell networks: comparison between the UHF/SHF and the millimetre wavebands

Emanuel Teixeira[1], Sofia Sousa[1], Fernando J. Velez[1], and Jon M. Peha[2]

[1]Instituto de Telecomunicações –DEM Universidade da Beira Interior, Faculdade de Engenharia 6201-001 Covilhã, Portugal, d1657@ubi.pt, sofia.sousa@lx.it.pt, fjv@ubi.pt
[2]Dept. of Electrical and Computer Engineering, Dept. of Engineering & Public Policy, Carnegie Mellon University, Pittsburgh, PA 15213-3890, USA peha@cmu.edu

Key Points:

- Urban/vehicular, pedestrian, urban micro and modified Friis propagation models have been considered for the UHF/SHF and millimetre wavebands.
- In the linear and Manhattan grid topologies, for short cell sizes, the supported throughput, which is mapped to the signal-to-interference-plus-noise ratio, is higher at the millimetre wavebands compared to the UHF/SHF bands.
- In the UHF/SHF band, for larger cell sizes/radius, all of the models are similar, but for shorter cell sizes, the number of needed pico cells is underestimated if the two-slope propagation model is considered instead of a single-slope model.

Corresponding author: Fernando J. Velez, `fjv@ubi.pt`

Abstract

This work shows how both frequency and the election of path loss model affect estimated spectral efficiency. Six different frequency bands are considered, ranging from 2.6 GHz in the Ultra High Frequency (UHF) band to 73 GHz in the millimetre wave bands (mmWaves), using both single-slope and two-slope path-loss models. We start by comparing four urban path loss models for UHF: the urban/vehicular and pedestrian test environment from the ITU-R M. 1255 Report, which includes the two-slope urban micro line-of-sight (LoS) and NLoS, from the ITU-R 2135 Report. Then, we consider mmWaves taking into consideration the modified Friis propagation model, followed by an analysis of the throughput for the 2.6, 3.5, 28, 38, 60 and 73 GHz frequency bands. We have found that the signal-to-interference-plus-noise ratio, as estimated with the more realistic two-slope model, is lower for devices that are within the break-point of the transmitter, which is a small distance in the UHF/SHF band. As a result, spectral efficiency is higher with mmWaves than with UHF/SHF spectrum when cell radius is under 40 meters but not when cells are larger. Consequently, mmWaves spectrum will be more valuable as cells get small. We also find that capacity as estimated with the two-slope model is considerably smaller than one would obtain with the one-slope model when cells are small but there is little difference in the models when cells are larger. Thus, as cells get smaller, the use of one-slope models may underestimate the number of cells that must be deployed.

1 Introduction

5G New Radio (NR) is a commercial technology with a service-based modular architecture *3GPP2015* [2015]. Its description in Rel. 15 of the Third Generation Partnership Project (3GPP) encompasses the underlying network functions (NFs) and offers services via a common framework that facilitates communications with data rates up to 2 Gbps *3GPP2015* [2015]. 5G is backward-compatible with LTE/LTE-A in the non-standalone stage. Their cellular infrastructure can offer different or equal coverage. Within 5G NR positioning scenarios, amongst supplementary topologies, it is conceivable to have an LTE/LTE-A eNB (evolved NodeB) as a master node, offering an anchor carrier that can be enhanced by a NR Next-generation NodeB (gNB), with data flow supported by the evolved packet core (EPC) *LiandJiang* [2017]. The physical layer process of NR is grounded on Orthogonal Frequency Division Multiplex (OFDM) through cyclic prefix (CP) both in the downlink and uplink directions. Uplink communication correspondingly utilizes Discrete Fourier Transform-spread-OFDM (DFT-s-OFDM). Both channels are intended to be bandwidth-agnostics *3GPP5GNR* [2017], with their capacity determined by the number of allocated physical resource blocks (PRBs), which in turn depends on the operating bandwidth and the sub-carrier spacing (SCS) *PRBs*. As defined by 3GPP Rel. 15, the sub-frames of NR are composed of slots that comprise 14 OFDM symbols, with lengths of 1 ms and 15 kHz sub-carrier spacing (SCS).

Recent work discloses that worldwide mobile data consumption will perceive the growth in coming years *JuandRappaport* [2018]. Due to the high awareness among the society in perceiving and predicting radio-propagation characteristics in several urban and suburban areas, it is very helpful to reach the capability of determining optimum 5G New Radio base-station locations, obtaining suitable data rates and estimating their coverage, without leading sequences of propagation measurement, which are costly and time overwhelming *Mollel* [2014].

In this work we compare the ITU-R 2135 model, *ITU-R* [2009] applied to the Urban micro (UMi) scenario, Line-of-Sight (LoS) or Non-Line-of-Sight(NLoS), and the Urban/Vehicular and Pedestrian models, defined in the ITU-R M.1255 Report applied to small cells (SCs), *ITU-R* [1997]. This is known as the UMi-A model. It captures the two-ray two-slope behaviour below 6 GHz *ITU-R2015* [2015]. In the millimetre wavebands (mmWaves), we only consider the modified Friis propagation model, with shadow fad-

ing. This model is also known as the UMi_B model *ITU-R2017* [2017] or close-in free space *Rapp15mmwbook* [2015] and *ITU-R2015* [2015], and represents one of the parts of a two-slope model for the millimetre wavebands applied to small cells, where the coverage and reuse distances are clearly shorter than the breakpoint distance. To understand the differences between lower and upper-frequency bands, we compare the system capacity, measured by the supported throughput, for small cells with coverage distance of a few hundred meters.

This work is an extended version of the URSI GASS 2017 paper *Sousa* [2017] paper shows the impact of path loss model on the capacity of small cells in the system capacity of small cell (SC) networks in the Ultra High Frequency (UHF)/ Super High Frequency (SHF) bands but also at the comparison between the UHF/SHF bands and the millimetre wavebands.

The system capacity is determined while considering the UHF/SHF and millimetre wavebands, where the frequency bands are the 2.6 and 3.5 GHz, as well as 28, 38, 60 and 73 GHz based on the analysis of the signal-to-interference-plus-noise ratio (SINR) within ubiquitous pico-cells (which interfere with each other). The computation of the SINR is performed within the framework of 5G New Radio (NR) mobile networks, considering a symmetrical hexagonal cell plan for UHF/SHF bands and linear topology in the mmWaves.

Rel. 15 has also established two groups of frequencies, labelled as frequency range 1 (FR1) and frequency range 2 (FR2) in *3GPPTS36212* [2013]. FR1 comprises the sub-6 GHz frequency range (450-6000 MHz) while FR2 is the mmWaves (24250-52600 MHz). In this work, we consider carrier frequencies within FR1 and FR2. Aiming at mapping the minimum SINR, ($SINR_{min}$), into the supported throughput, R_b, the values for $SINR_{min}$ from 3GPP *3GPPTS36212* [2013], *3GPPTS38214* [2018], *3GPPTS38104* [2020], *5GNRAhmadi* [2019] and *5GNRDahlman* [2018].

The remainder of the paper is organized as follows. Section 2 gives an overview of the considered propagation models and their application to the analysis of the frequency reuse trade-off. Section 3 estimates the SINR for different topologies and the frequency reuse is compared between different frequency bands. In section 4, the supported throughput is analysed, by comparing the results between the single-slope and two-slope models in the UHF/SHF bands, and by understanding the behaviour among different frequencies in the mmWaves, e.g., the impact of the oxygen absorption at 60 GHz. Finally, conclusions are drawn in Section 5, where suggestions for future research are also discussed.

2 Overview of the propagation models

Numerous propagation path loss models have been developed and proposed for cellular systems operating in different environments (outdoor, urban, suburban, rural, and indoor). However, the scientific community as in *Hanedaetal* [2016] argue that for the development of new 5G systems operating in bands above 6 GHz, the propagation models for these new systems, requires to be appropriate for higher frequencies, due to the fact that the preceding generation of channels models were planned for frequencies up to 6 GHz.

The path loss model represents the reduction of the signal when it is propagating from the transmitter to the receiver, i.e., between the base station (or gNB) and mobile user. The propagation models can be deterministic, stochastic or empirical *AbhandWass* [2005]. The deterministic model considers a specific transmitter location, a receiver location, and the properties of the environment. This type of model uses electromagnetic wave propagation and requires the 3-D map of the propagation environment. In many cases, it is not possible to consider such a specific environment, and the appropriate ap-

proach is to consider channels that model the " typical", "worst-case" or "best-case" *IEEE* [2009]. One example of the deterministic model is a ray tracing model. The stochastic models represent the environment as a sequence of arbitrary variables, consequently demanding less information about the environment and the use of less processing power. An empirical model is based on measurements. The respective classification of empirical models can be further divided into time dispersive and non-time dispersive. Time dispersive provides information about time dispersive characteristics of the channel, i.e., the multipath delay spread of the channel. Non-time dispersive consider various parameters, such as distance, antenna heights, frequency and transmitter power to predict average path loss, from ITU-R introduces the urban micro, UMi_A and UMi_B, models, and considers two-slope models to be applied in different small cell environments *ITU-R2017* [2017].

International Telecommunication Union - Radio communication Sector (ITU-R) was also responsible for defining a global standard for the fourth generation of mobile communication systems known as international mobile telecommunications (IMT) – Advanced *LTE* [2014] and a global standard for 5G, known as IMT 2020, *IMT2020* [2013].

This Section gives insights on the propagation models applied to small cell environments for the UHF/SHF bands and millimetre wavebands. On the one hand, The ITU-R M.1225 Report has provided guidelines for assessing several test environments in the UHF/SHF bands. The scenarios under study are the outdoor-to-indoor/pedestrian test environments and vehicular test environment. Outdoor-to-indoor and pedestrian test environments are characterized by small cells and low transmitter power. Base stations with low antenna heights are located outdoor. Pedestrian users are situated on streets, inside buildings and residences. As such, the vehicular test environment is characterized over larger cells and higher transmitter power. The path loss model defined in the ITU-R M.2135-1 Report suggests models that represent the channel behaviour via deterministic category. The deterministic category comprehends all models that describe the propagation channel for specific transmitter and receiver positions. The two-slope behaviour can certainly be captured by a deterministic procedure, as ray tracing. However, the complexity of its application does not facilitate its use into cellular optimization or planning tools where it is easier to apply a less complex empirical model. For the valuation of the IMT-Advanced candidates, the ITU-R WP D describes several test environments *ITU-R* [2009]. The assessments in this study consider the microcellular scenario. The microcellular test environment focuses on small cells, high user densities and traffic loads in city centres and dense urban areas. The key features of this test environment are high traffic loads, along with the outdoor and outdoor-to-indoor coverage. In this work, the channel model for urban micro-cell scenario is called urban micro (UMi) and is being considered for picocellular systems, where the models can be applied in the 2-6 GHz frequency range *ITU-R* [1997]. As discussed above, system planning requires new channel models that fit the intended frequency range to produce accurate performance. Thus, the propagation models must be accurate up to frequencies of 6 GHz, allowing truthful performance assessment of conceivable new specifications, innovative environments and scenarios of interest for 5G systems. Accordingly, the above-mentioned models ought to be reliable with the models for frequencies up to 6 GHz. Some models are deviations from the specifications of the prevailing models. Several researchers *Hanedaetal* [2016] from around the world have been proposing and testing these models. Examples are as follows: WINNER II *MacCartneyandRappaport* [2013], IMT- A *MacCartneyandRappaport* [2013], METIS2020 *METIS* [2015], COST2100/COST *cost2100* [2012], IC1004 *ic1004* [2012], ETSI mmWave *ETSI* [2015], NIST 5G mmWave Channel Model Alliance *NIST* [2016], MiWEBA *MiWEBA* [2014], mmMagic *mmMagic* [2017], and NYU WIRELESS *RappaportandSun* [2013], *Rapp15mmwbook* [2015], *RappaportandMacCartney* [2015], *MacCartneyandRappaport* [2015]. WINNER I is intended for use with the 2 - 6 GHz frequency band. It resulted in two frequently-used channel models for designing 4G networks, specifically the 3GPP/3GPP2 Spatial Channel Model (3GPPSCM) and the IEEE 802.11n channel model *BaumandSalo* [2005].

The WINNER I channel model encompasses an extensive variety of propagation scenarios: indoor, urban microcell, urban macrocell, suburban macrocell, rural macrocell, and stationary feeder links *MacCartneyandRappaport* [2013]. The WINNER II model is an enhancement of the WINNER I model and considers a number of scenarios, including indoor-to-outdoor, outdoor-to-indoor, and bad urban microcell *MacCartneyandRappaport* [2013]. Due to the accuracy of the WINNER II model in forecasting large scale path loss statistics, it has been extensively applied for 3G and 4G channel model design *IST-WINNER* [2007]and at microwave frequencies. However, the model lacks the temporal resolution to model or simulate future multi-Gigabit/s wireless links with ultra-low latency *MacCartneyandRappaport* [2013]. WINNER II is a geometry-based stochastic channel model (GSCM) that is parametrized for many scenarios at the microwave frequencies, targeting the reproduction of the physical parameters of plane waves from statistical distributions of the channel parameters. The physical parameters comprise angles of departure and arrival and delay of each plane wave seen from the transmitter and receiver antennas *KarttunenandJarvelainen* [2015].

METIS2020 is dedicated to 5G technologies and has broadly contributed to channel modelling studies over a wide range of frequency bands (up to 86 GHz), very large bandwidths, three-dimensional polarization modelling, spherical wave modelling, and high spatial resolution, involving of a map-based model, stochastic model, and a hybrid model which can meet flexibility and scalability requirements*Hanedaetal* [2016]. The International Mobile Telecommunications-Advanced (IMT- A), evolved from the IMT-2000 system. In the IMT-A urban microcellular channel model, users are randomly and uniformly distributed *ETSI* [2015]. The COST2100 is a geometry-based stochastic channel model (GSCM) that can reproduce the stochastic properties of multiple-input/multiple output (MIMO) channels over time, frequency, and space *Hanedaetal* [2016]. The NIST 5G mmWave Channel Model Alliance is proposing procedures for measurement calibration and methodology, modelling methodology, as well as parametrization in various environments and a database for channel measurement campaigns *Hanedaetal* [2016]. NYU WIRELESS has led wide propagation measurements at 28, 38, 60, and 73 GHz for both outdoor and indoor channels, and has shaped large-scale and small-scale channel models, including the concepts of time cluster spatial lobes (TCSL) to model multiple multipath time clusters that are seen to arrive in particular directions campaigns *RappaportandSun* [2013], *Rapp15mmwbook* [2015], *RappaportandSamimi* [2015].

On the other hand, in the millimetre wavebands, in Line-of-Sight (LoS), we have considered the modified Friis propagation model with shadow fading. It is an ideal model that does not consider any obstacles. Diverse authors express that LoS path loss for frequency bands higher than 6 GHz can be represented by Friis' free space path loss model, which is also well employed as well in lower bands *Rapp96book* [1996], *VelezandBrazio* [1996] . The shadow fading in the assessments seem to be comparable between different frequencies bands up to 6 GHz, whereas ray tracing yields higher shadow fading ($>$ 10 dB) than measurements, due to the larger dynamic range permitted and higher loss in ray tracing research *Hanedaetal* [2016]. The propagation exponent is $\gamma = 2.1$ at 28 GHz, and $\gamma = 2.3$ at 38 GHz, 60 GHz and 73 GHz from *Rapp15mmwbook* [2015]. In the application of mmWave bands for longer range, NLoS cellular scenarios are a new boundary. The viability of such systems has been the subject of substantial discussion, as presented by *RanganandRapp* [2014]. A comparison between UHF/SHF and mmWaves is thus in order. As propagation happens essentially in LoS, the shape of the cells and co-channel interference are determined, to a vast extent, by the location of the nearby objects, in particular buildings (in urban outdoors scenarios). Subsequently, for cellular design purposes, easy analytical treatment is only possible for environments with a regular structure, like the linear and the 'Manhattan grid' (planar regular) geometries *FJV* [2000].

2.1 Characterization of the Propagation Models in the UHF/SHF bands

The propagation physiognomies for the outdoor-to-indoor/ pedestrian (***Ped***) test environment are characterized by the following path loss model, valid in the UHF/SHF bands, more specifically in the range between 2 and 6 GHz, as proposed in *ITU-R* [2009], *ITU-R2017* [2017]

$$PL_{Ped} = 40 \cdot log_{10}(d_{[km]}) + 30 \cdot log_{10}(f_{[MHz]}) + 49 \quad (1)$$

where d is the separation between the mobile and base stations, in km, and f is the carrier frequency, in MHz.

The path loss for the vehicular/urban (***Urb***) test environment is characterised by the following model:

$$PL_{Urb} = 40 \cdot (1 - 4 \cdot 10^{-3} h_{BS[m]}) \cdot log_{10}(d_{[km]}) - 18 \cdot log_{10}(h_{BS[m]}) + 21 \cdot log_{10}(f_{[MHz]}) + 80 \quad (2)$$

where h_{BS} is the base station antenna height, in m, measured from the average rooftop level.

For instance, for $f = 2.6$ GHz and $h_{BS} = 10$ m, the path loss, in dB, is given by:

$$PL_{Ped} = 40.0 \cdot log_{10}(d_{[km]}) + 151.45 \quad (3)$$

$$PL_{Urb} = 38.4 \cdot log_{10}(d_{[km]}) + 133.71 \quad (4)$$

The UMi outdoor scenario is characterized by the following two-slope path loss model:

$$PL_{UMiLoS} = 22 \cdot log_{10}(d_{[m]}) + 28.0 + 20 \cdot log_{10}(f_{c[GHz]}),\ 10\ m < d < d_{BP} \quad (5)$$

$$PL_{UMiLoS} = 40 \cdot log_{10}(d_{[m]}) + 7.8 - 18 \cdot log_{10}(h'_{BS}) - 18 \cdot log_{10}(h'_{UT}) + 2 \cdot log_{10}(f_{c[GHz]}),\ d_{BP} < d < 5000\ m \quad (6)$$

$$PL_{UMiNLoS} = 36.7 \cdot log_{10}(d) + 22.7 + 26 \cdot log_{10}(f_{c[GHz]}) \quad (7)$$

where $h_{BS} = 10$ m and the considered street width is 20 m, while the average building height is 20 m. Variables $h'_{BS[m]} = h_{BS} - 1$ and $h'_{UT[m]} = h_{UT} - 1$ also stand. The breakpoint distance, d_{BS}, is calculated by:

$$d_{BP} = 4 \cdot h'_{BS} \cdot h'_{UT} \cdot f_c / c \quad (8)$$

where f_c is the centre frequency, in hertz, c=3.0 x 10^8 m/s is the propagation velocity in free space. The ITU-R proposes to consider the two-slope propagation model that accounts for two-path fading, which happens for longer distance, to optimize small cells in urban micro Line-of-Sight (UMiLoS) environments. S. Min and H. L. Bertoni identified that, as a result of the two-slope behaviour, smaller out-of-cell interference is obtained with the two-slope model, leading to, according to *MinandBertoni* [1998], system designs with different optima than are obtained using the single-slope model. Therefore, one obtains $d_{BPUMiLoS} = 156$ m. By considering these assumptions, the path loss, in dB, is given by:

$$PL_{UMiLoS}(d) = 22 \cdot log_{10}(d_{[m]}) + 36.30, d < 156\ \text{m} \quad (9)$$

$$PL_{UMiLoS}(d) = 40 \cdot log_{10}(d_{[m]}) - 3.13, d \geqslant 156\ \text{m} \quad (10)$$

$$PL_{UMiNLoS}(d) = 36.7 \cdot log_{10}(d_{[m]}) + 33.48 \quad (11)$$

For a noise temperature $T = 293$ K, the noise power at the receiver is calculated by:

$$N_{[dBm]} = -174 + 10 \cdot log_{10}(BW_{[Hz]}) + N_{f[dB]} \quad (12)$$

where BW is the bandwidth and N_f is the noise figure at the receiver. In the UHF/SHF bands the assumed gains are $G_t = 17$ dBi and $G_r = 0$ dBi, the transmitter power are P_t = -7 dBW for 2.6 GHz and P_t = -4.75 dBW for 3.5 GHz . The following parameters are also considered: $BW = 20$ MHz and $N_f = 5$ dB *ITU-R* [2009], *Sousa* [2017], *Silva* [2018].

2.2 Propagation Models in the Millimetre Wavebands

In the millimetre wavebands, in Line-of-Sight (LoS), the path loss is defined by the following equation:

$$PL_{LoS}\ [_{dB}]\,(d) = 20 \cdot log_{10}\left(\frac{4\pi}{\lambda}\right) + \bar{n} \cdot 10 \cdot log_{10}\ \left(d_{[m]}\right) + X_{\sigma}, d \geqslant 1m \tag{13}$$

where X_{σ} models the shadow fading and is the typical log-normal random variable with 0 dB mean and standard deviation σ, in decibels. The power and gains are P_t = -17 dBW, G_t = 15 dBi and G_r = 0 dBi, respectively. In order to compare the UHF/ SHF and millimetre wavebands, the assumed bandwidth is BW = 20 MHz while the noise figure is N_f = 7 dB *Rapp15mmwbook* [2015], *FernandesandBarbosa* [1995], *VelezandBrazio* [1996] (where P_t = -17 dBW; N.B.: 20 mW is the maximum effective isotropic radiated power, EIRP, power in Europe and 500 mW in USA *Rapp15mmwbook* [2015]). In the millimetre wavebands, the breakpoint distance takes place at long distances. As such distances does not correspond to SCs, in this paper we do not explore them.

3 Pico Cellular System

In this section, we define the topology of the pico cellular system, and how to compute the cell coverage range for planning and frequency assignment purposes. We determine the carrier-to-interference ratio (C/I) and signal-to-interference-plus-noise ratio (SINR) in Orthogonal Frequency Division Multiplexing (OFDM) system with static allocation scheme, or fixed channel allocation. We consider a symmetrical hexagonal cell plan for UHF/SHF bands, and linear topology in the mmWaves, as shown in Figure 1 (a) and (b) , respectively. The use of dynamic Modulation and Coding Schemes (MCSs) implies that each MCS requires a minimum SINR. Coverage planning and optimization are necessary to guarantee the quality of the received signal for both the downlink (DL) and uplink (UL). One of the objectives is to design a wireless network where, for given available bandwidth and different cell sizes, the system capacity trade-off is optimized.

3.1 Frequency Reuse in the UHF/SHF Bands

We address the downlink, where, the (UE) is at the cell edge, and frequency reuse three is considered, for the worst-case situation.

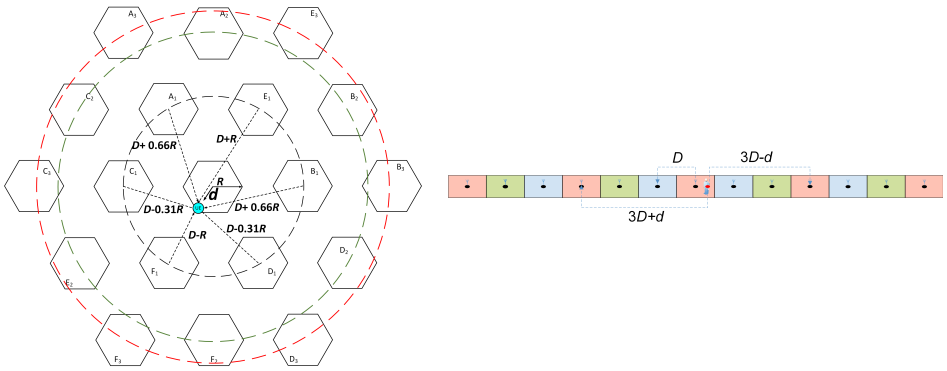

(a) Hexagonal cellular topology, for UHF/SHF bands, where the first and second tiers of co-channel interference are represented

(b) Linear cellular topology, for mmWaves.

Figure 1: Scenario in the UHF/SHF and millimetre wavebands.

In a fully symmetrical hexagonal plan, with a given frequency reuse pattern K, we consider the reuse distance, $D{=}\sqrt{3K}R$, where R is the radius of the hexagonal cell. The possible values for reuse pattern are $K = 1, 3, 4, 7$, where $K = 1$ is the case where all channels are used in all cells (for UHF/SHF bands). As for the very short coverage distances associated with small cells, the approximate C/I formulation considered in the previous works *FJVetall* [2016] has shown to be unfitting, a comprehensive approach is sought in this work.

For UHF/SHF bands, the carrier to interference ratio formulation used in a previous work from *Sousa* [2017] is given by the following equation:

$$\frac{C}{I} = \frac{1}{2(r_{cc}+1)^{-\gamma} + 2{r_{cc}}^{-\gamma} + 2(r_{cc}-1)^{-\gamma}} \approx \frac{{r_{cc}}^{\gamma}}{6} \tag{14}$$

where r_{cc} is the co-channel reuse factor, given by $r_{cc} = D/R$.

In this work, we have obtained a more detailed equation that represents C/I with exact values of the interference to the UE for all the reuse distances, from the gNBs of the first, second and third tiers of co-channel cells (interferers). In these equations, we consider the exact position of each interferer, in each tier of interference, in opposition to the equations with approximate values for the reuse distances.

With hexagonal cell topologies for the macro- and pico- cellular layers, in the DL, for $K = 3$, the carrier-to-interference-ratio is given by the following equations for the 1^{st}, 2^{nd} and 3^{rd} rings of interference, respectively:

$$\frac{C}{I}_{1^{\text{st}}} = \frac{R^{-\gamma}}{2(D+0.66394R)^{-\gamma} + 2(D-0.31395R)^{-\gamma} + (D+R)^{-\gamma} + (D-R)^{-\gamma}} \tag{15}$$

$$\frac{C}{I}_{2^{\text{nd}}} = \frac{R^{-\gamma}}{2\left(\sqrt{3}D+0.88915R\right)^{-\gamma} + 2\left(\sqrt{3}D+0.8591R\right)^{-\gamma} + 2\left(\sqrt{3}D-0.84799R\right)^{-\gamma}} \tag{16}$$

$$\frac{C}{I}_{3^{\text{rd}}} = \frac{R^{-\gamma}}{2(2D+0.55802R)^{-\gamma} + 2(2D+0.47727R)^{-\gamma} + (2D+R)^{-\gamma} + (2D-R)^{-\gamma}} \tag{17}$$

Considering the first three tiers of interferers is a valid approximation, since the interference obtained from the second and third tiers, the interference is very low compared to the previous tiers, respectively.

3.2 Frequency Reuse in the Millimetre Wavebands

In the mmWaves, the main streets from the Manhattan grid topology LoS are considered. In the downlink, the worst-case SINR is comparable to the worst-case SINR from the linear cellular topology, from 1 (b). SINR is higher for Manhattan topology compared to the linear topology. However, this is only noticeable if the UE is positioned at distances shorter than half of the street length, as shown in Figure 2 from *Teixeira* [2018] and *TeixeiraandVelez* [2019]. Henceforth the linear topology can be considered instead for the reason that in the Manhattan topology when the UE is located at distances longer than half of the street length from the gNBs, there are only two cells of interference. As such, the linear topology can be considered in SINR computations, as it adequately represents the Manhattan grid topology with reasonable details.

The carrier-to-interference-ratio formulation in the linear topology, is given by the following equation, where the first and second rings of interference have been considered:

$$\frac{C}{I} = \frac{d^{-\gamma}}{(3D-d)^{-\gamma} + (3D+d)^{-\gamma} + (6D-d)^{-\gamma} + (6D+d)^{-\gamma}} \tag{18}$$

The UE is at a distance d from the central gNB ($0 \leq d \leq R$). It is worthwhile to note that, in the mmWaves and linear topology, the second ring of interference can be neglected for reuse pattern $K = 3$. In particular, it can be neglected, at 60 GHz, as the oxygen attenuation excess is relevant for the longest distances.

3.3 Frequency Reuse Trade-off

For comparison purposes, we consider the linear topology. However, to facilitate a link to the previous work, in the UHF/SHF bands results for the hexagonal topology are still considered. In order to compare all the frequency bands, we have considered the hexagonal and linear topologies in the computations of the SINR. By considering the above formulations and 20 MHz bandwidth, Figures 2, 3 present the variation of the SINR with the distance, d, from the cell centre to the UE within a cell for cell coverage radii $R =$ 30 and 300 m, where $0 \leq d \leq R$. The behaviour of the SINR is similar for all frequency and scenarios, except for the UMi LoS scenario (2.6 and 3.5 GHz). In UMi LoS scenario, a slight inflection point is observed at the breakpoint distance. The 2.6 GHz Umi NLoS show higher SINR than UMi LoS at short distances by applying UMi NLoS, obtained SINR, is higher than with UMi LoS, at short distances. Due to the higher attenuation when C/I is lower, the resulting SINR is lower. In practice, this effect is more evident, because overall, the probability of having NLoS at long distances is higher. Meanwhile the propagation exponent is $\gamma = 2.2$ for shortest coverage distances, the SINR is considerably lower, as shown in Figures 2 (a) and 3 (a). For Rs longer than d_{BP}, since the propagation exponent for UMi LoS is now $\gamma = 4$, the obtained SINR is higher than the one obtained for the single-slope path loss models, as shown in Figure 2 and 3. For UMi NLoS, Urban and Pedestrian environments, the respective propagation exponents are $\gamma = 3.67$, 3.84 and 4. *ITU-R* [2009], *Sousa* [2017]. The propagation exponent for mmWaves is $\gamma = 2.1$ for the 28 GHz band and $\gamma = 2.3$ for 38, 60, 73 GHz *Rapp15mmwbook* [2015]. For long distances, the obtained SINRs for mmWaves are lower than for the UHF/SHF bands. On the one hand, at 30 m, for linear topology, the difference in the values of SINR between the 28 GHz and the Umi LoS is less 4 dB. On the other hand, at 300 m, the difference in the values of SINR between the 2.6 GHz - Umi LoS and the 60 GHz (the lowest SINR) is circa than 30 dB on average.

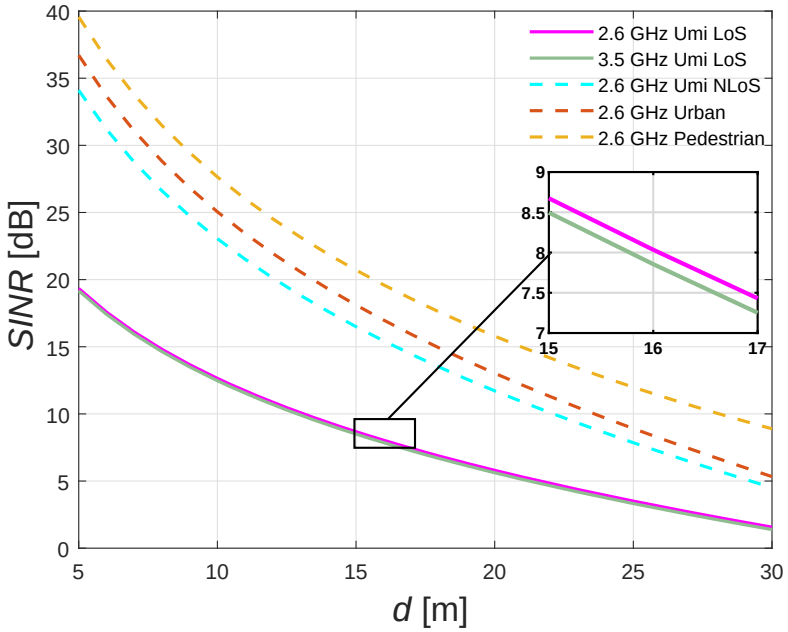

(a) K=3 and R=30 m

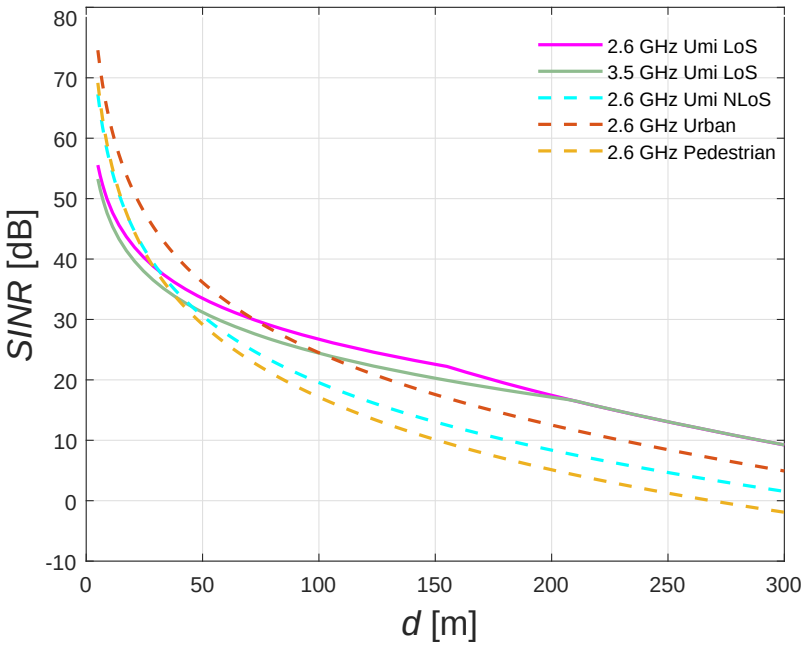

(b) K=3 and R=300 m.

Figure 2: Comparison of SINR between the UMi LoS, UMi NLoS, Urban and Pedestrian, propagation models at the 28 GHz, 38 GHz, 60 GHz and 73 GHz frequency bands, for the hexagonal topology, and different cell sizes.

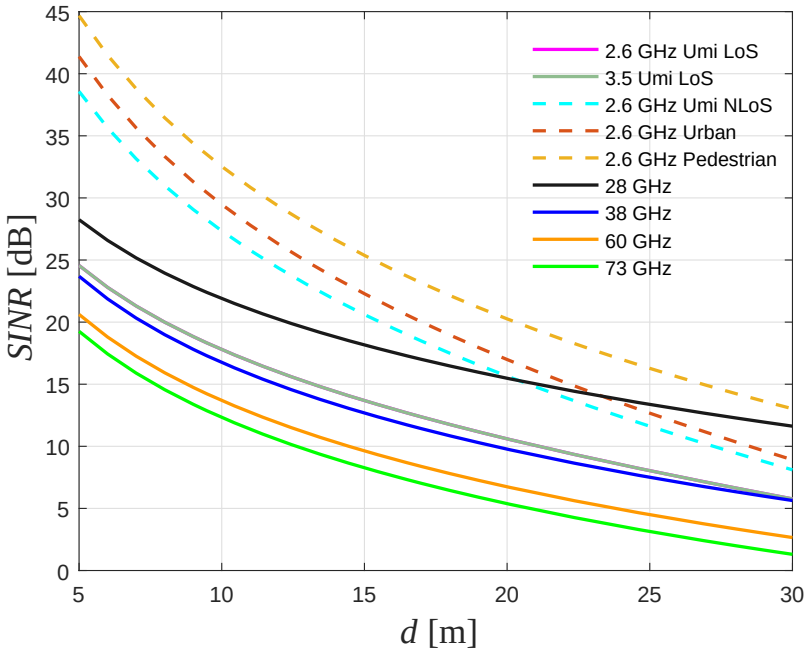

(a) R=30 m.

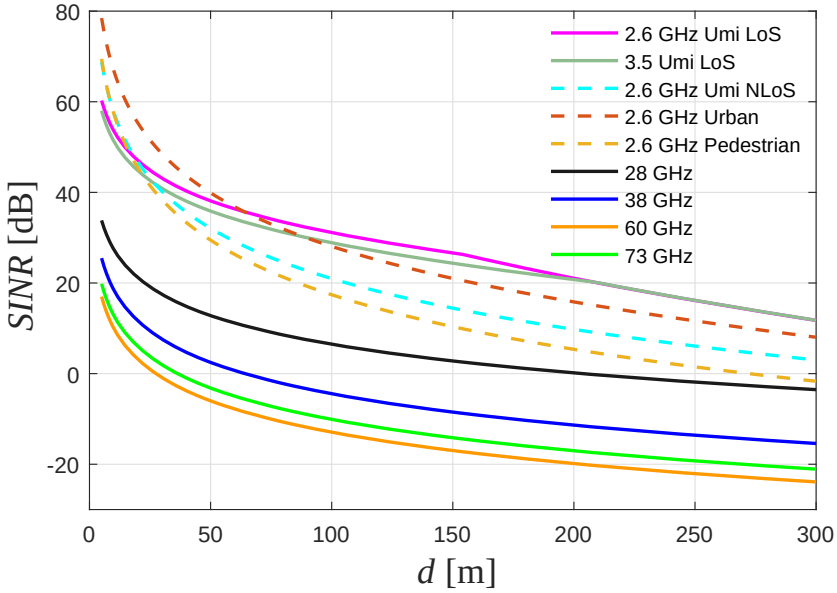

(b) R=300 m.

Figure 3: Comparison of SINR between the UMi LoS, UMi NLoS, Urban and Pedestrian, propagation models with 28 GHz, 38 GHz, 60 GHz and 73 GHz frequency bands, for the linear topology.

4 Supported Cell Throughput

As a measure of system capacity, it is worthwhile to analyse the behaviour of the supported cell throughput, it is obtained as *PrasadandVelez* [2010]:

$$R_{b\_sup} = \sum_{i=1}^{n} \frac{R_{b_i}(d_i^2 - d_{i-1}^2)}{R^2} \tag{19}$$

It is computed by weighting the PHY throughput in each coverage ring (different hexagonal/rectangular *crowns*) by the size of the ring where that value is supported, where R is the cell radius and n as the respective number of coverage rings. The contribution of each of the transmission modes is thus considered. The LTE-A system capacity is analysed by the implicit function formulation to compute the supported cell throughput, R_{b-sup} from *RobaloandFJV* [2015]. This analysis considers the different values of the reuse pattern, e.g., $K = 3$. To map the minimum signal-to-interference-plus-noise ratio, $SINR_{min}$, into the supported throughput, R_b, we have used the values for $SINR_{min}$ from *3GPP* [2013]. By extrapolating the gathered information, it is possible to map the $SINR$ into MCS index, Modulation Order Transport Block Size (ITBS) index and TBS.

4.1 Comparison between one-slope and two-slope models

Regarding the UMi LoS propagation model, figure 4 (a) presents the results for the supported throughput per cell, R_{b-sup}, for the hexagonal topology. Figure 4 (b) presents the results for R_{b-sup} for the linear topology, for cells with Rs shorter than 300 m.

The values of the supported throughput are similar between 2.6 and 3.5 GHz for Rs up to circa 50 m. However, for coverage distances longer than 50 m, lower values of the supported throughput occur at 3.5 GHz for both topologies. We can observe that, after some distance, at 2.6 and 3.5 GHz, the supported throughput becomes different for the longest coverage distance, and the system becomes noise limited (not interference limited anymore). As coverage is better at the 2.6 GHz frequency band (compared to 3.5 GHz band), the supported throughput becomes higher and higher for the lowest frequency band.

For cells with the shortest Rs, more optimistic results are obtained with the Pedestrian path loss model, followed by the Urban and UMi NLoS propagation models.

The UMi LoS model presents the most pessimistic results for small cell coverage ranges. Nevertheless, for longer cell ranges, the best results for the cell supported throughput are obtained for UMi LoS, followed by the Urban, Pedestrian and UMi NLoS models.

4.2 Comparison between UHF/SHF and mmWave bands

Figure 5 (a) presents the results for the R_{b-sup}, for the UHF/SHF and mmWaves considering the modified Friis propagation model (28, 38, 60, 73 GHz) and the UHF/SHF considering the UMi LoS propagation model (2.6 and 3.5 GHz).

The comparison between UHF/SHF and mmWaves is only made for the linear topology and the two-slope model, i.e., the UMi LoS model. The approach of the linear geometry is found in the worst case that bounds the SINR from a Manhattan grid topology in the mmWave bands, as discussed in *Teixeira* [2018].

For cells with the shortest Rs, higher supported throughput is obtained for the modified Friis propagation model applied to mmWaves at 28 GHz (achieving circa 180 Mbps), followed by the curves for the UMi LoS model (2.6 and 3.5 GHz) and then the 38, 60 and 73 GHz. At $R \approx 40$ m the curve for 2.6 and 3.5 GHz begins to overcome the sup-

ported throughput of the 28 GHz curve, reaching more than 210 Mbps for the longest Rs.

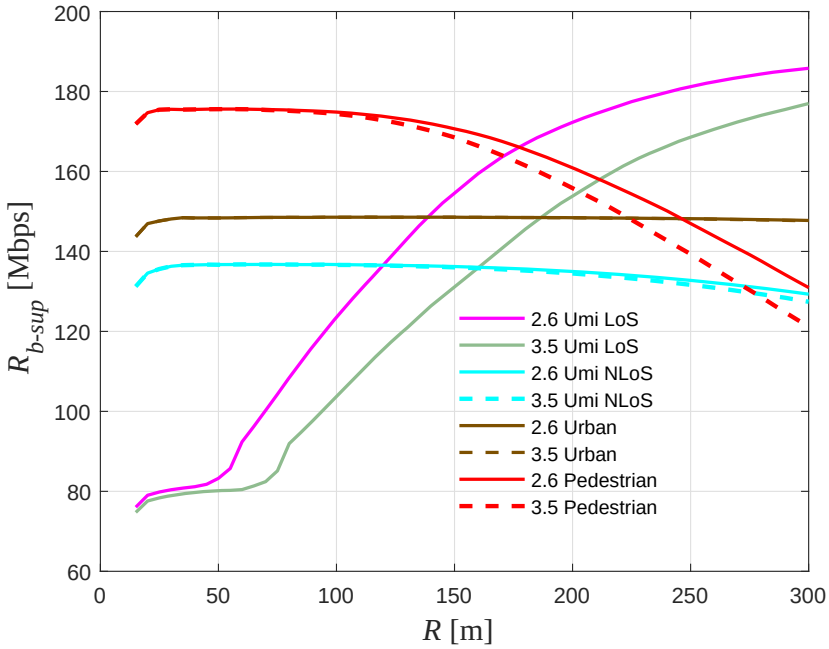

(a) Hexagonal topology

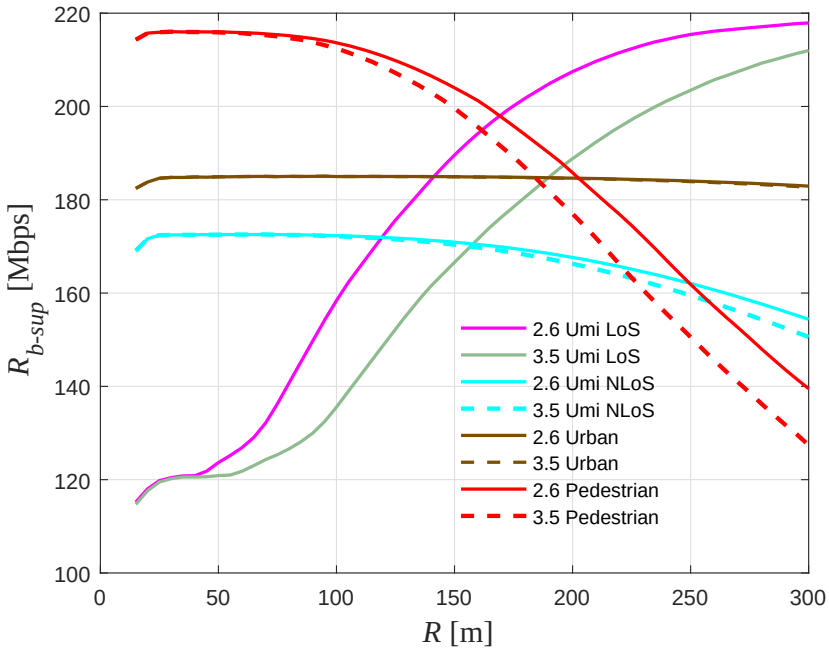

(b) Linear topology

Figure 4: Comparison of equivalent supported throughput between UHF/SHF and millimetre wavebands for $BW = 20$ MHz.

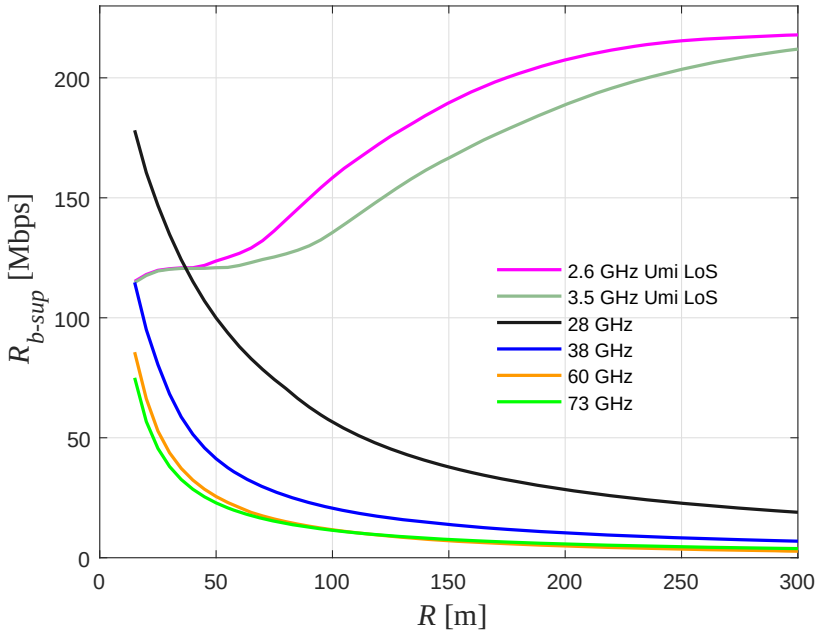

(a) Bandwidth = 20 MHz

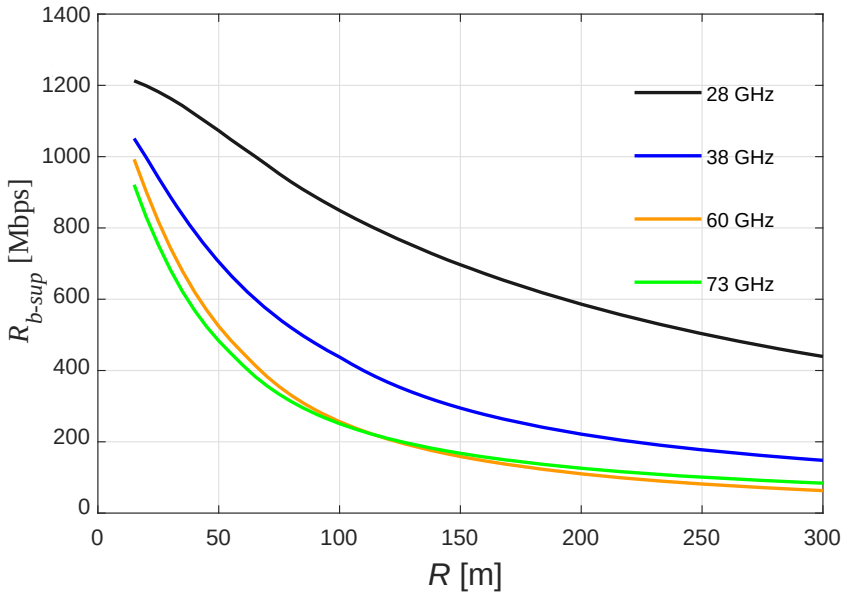

(b) Bandwidth = 100 MHz

Figure 5: Comparison of equivalent supported throughput between UHF/SHF and millimetre wavebands for the linear topology, for different bandwidths (for 100 MHz bandwidth only the millimetre wavebands are considered).

Overall, for short distances, in the mmWaves the supported throughput is higher at 28 GHz compared to the rest of the frequency bands. This is followed by the 2.6 and 3.5 GHz, 38 GHz and then the 60 GHz frequency band, which only performs better than the 73 GHz band for Rs up to approximately 120 m. Therefore, the supported throughput at 73 GHz is higher. This is due to attenuation caused by O_2 which causes a reduction in the coverage range at 60 GHz *Teixeira* [2018], when the system is interference limited, i.e, for shortest coverage distance. For the longest coverage distances the system is noise limited. Higher throughputs are achieved with mmWave spectrum over short distances, but UHF/SHF for UMi LoS achieves higher throughputs over longer distances.

N.B.: In the mmWaves we have compared the supported throughput per cell, R_{b-sup}, for different frequency bands, as shown in Figure 5 (a), but we have not compared different propagation models, while in the UHF/SHF we have compared propagation models for different scenarios, as shown in Figure 7. Considering different reuse patterns and considering the second ring of interference, the behaviour of the system is identical for all the studied cases. In our investigation, we have observed a slight reduction of the values, circa than 1 Mbps in terms of throughput, and less than 1 dB in terms of SINR in the analysis of the interference by the second ring. Considering higher reuse patterns, we have observed higher values for throughput and SINR. However, we have been restricted by the available operator's resources. Although typical bandwidths can differ across frequency bands, we have used a bandwidth of 20 MHz in all bands because we wish to make a fair comparison, and larger bandwidth, of the order of 100 MHz bandwidth, is not available in a contiguous way, in the lowest frequency bands. A bandwidth of 20 MHz that yields a total of 24 *PRBs* with 60 kHz SCS and for FR2 a bandwidth of 100 MHz that yields a total of 66 *PRBs* with 60 kHz SCS. In Figure 5 (b) we have considered 100 MHz, where more than 1200 Mbps can be achieved for the throughput at the 28 GHz frequency band, knowing that a similar behaviour of the supported throughput would be observed for the 20 MHz bandwidth.

4.3 Variation of the supported Throughput in the Pedestrian Scenario and UHF/SHF bands

To understand the impact of considering a more realistic propagation model that accounts for the existence of a breakpoint distance, in the behaviour of the path loss, in radio and network optimization, we analyse the supported throughput per unit area, R_{b-ua}, for hexagonal shaped (in the UHF/SHF bands) and linear cellular geometries, it is worthwhile to define the number of the cells per unit area (i. e., per square kilometre), $N_{C/ua}$, as follows:

$$N_{C/ua} = \frac{\frac{1}{2.R_{[km]} - \frac{w_{[km]}}{2}}}{l_{[km]}} \tag{20}$$

where w is the width and the l is the length of the street.

R_{b-ua} is obtained by multiplying the number of cells per unit area by the supported cell throughput.

The reduction of the supported throughput while considering the UMi LoS propagation, $R_{b-uaUMiLoS}$, is compared to the supported throughput for the Pedestrian propagation scenario. The values of the $R_{b-uaPed}$, allow for defining the reduction of the throughput, Red_{Rb-ua}, and is obtained by the following ratio:

$$Red_{Rb-ua}[\%] = \frac{R_{b-ua_{UMi_{LoS}}} - R_{b-ua_{Ped}}}{R_{b-ua}Ped} \cdot 100 \tag{21}$$

For $K = 3$, in Figure 7 we observe that, for cells with the shortest coverage distances, for example, $R = 50$ m, the supported throughput per unit area, R_{b-ua}, obtained for the two-slope model (UMi LoS) is reduced by 49.33 % compared to the results that arise from applying the single-slope model (Pedestrian scenario). For K=4, the two-slope model

has a reduction of 31.32 % in R_{b-ua} compared to the values obtained with single-slope model.

Figure 7 shows the ratio between R_{b-ua} for the two-slope model (UMi LoS) and R_{b-ua} for the one-slope model (Pedestrian), in percentage, i.e., Red_{Rb-ua}.

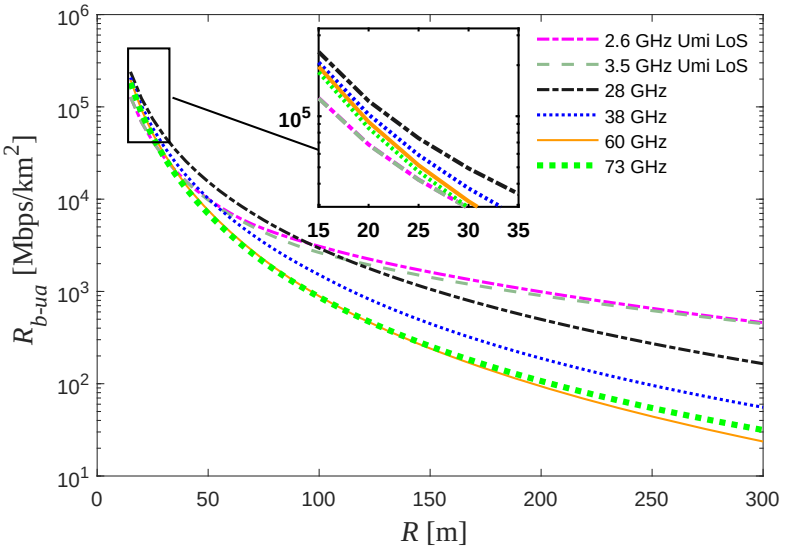

Figure 6: Comparison of the equivalent supported throughput per unit area between UHF/SHF and millimetre wavebands, for the linear topology.

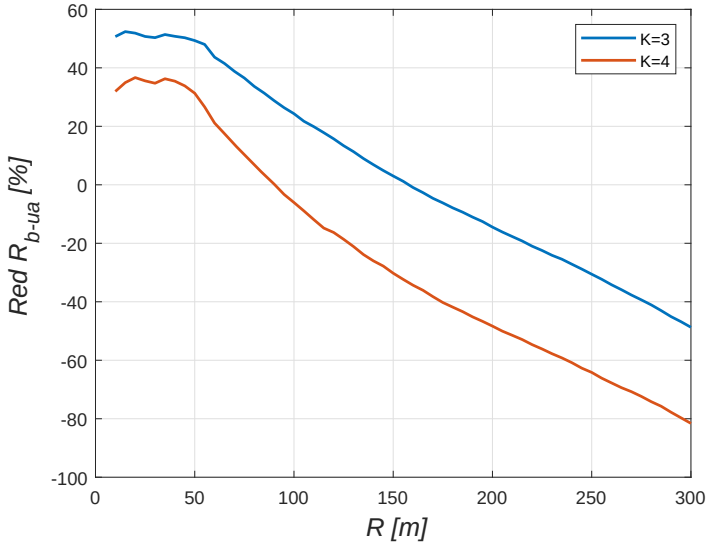

Figure 7: Reduction of the equivalent R_{b-ua} between the UMi LoS and Pedestrian path loss models, in percentage, for $K = 3$ and 4, $BW = 20$ MHz.

Results for the supported throughput with the two-slope model overcome the value obtained for R_{b-ua} from the one-slope model for coverage distances longer than $R \approx 156$ m and $R \approx 90$ m, for K=3 and 4, respectively. In fact, values of Red_{Rb-ua} higher than zero mean a reduction of the throughput when considering the two-slope model, whereas negative values (obtained for Rs longer than these values) mean that the single-slope models are more pessimistic in the determination of the supported throughput per unit area).

The two-slope model, whose break-point distance defines the change of the propagation characteristics, captures the actual behaviour of the propagation in small cell environments, From this analysis, we conclude that by considering the more-realistic ITU-R M.2135 UMi LoS propagation model, lower values of the throughput per unit area are achievable for shorter Rs while, for longer Rs, the consideration of the two-slope model leads to higher values of system capacity.

5 Conclusions

In this paper, the 5G cellular coverage and frequency reuse are studied based on the signal-to-interference-plus-noise ratio. Urban/vehicular, pedestrian, urban micro and modified Friis propagation models have been considered for the Ultra/Super High Frequencies and millimetre wavebands.

On the one hand, this work has evaluated the impact of considering different path loss models in the study of the frequency reuse and system capacity trade-off of small cell networks. In the UHF/SHF bands, we have obtained a detailed equation that represents the carrier-to-interference ratio, C/I, with exact values for all the reuse distances, from the gNBs of the first, second and third tiers of co-channel cells (interferers) to the UE.

We have learned from the analysis that by considering the realistic assumptions from the ITU-R two-slope, for coverage distances, R, up to the breakpoint distance divided by the reuse factor, d_{BP}/r_{cc}, the supported throughput R_{b-sup}, is much lower than expected when traditional single-slope models are assumed. For Rs longer than d_{BP}/r_{cc} the results for R_{b-sup} are increasing with R, whereas they are steady or decreasing with R while considering the traditional single-slope propagation models. This increase is due to the existence of a low propagation exponent (slope) in term of coverage and a high slope in terms of interference for $d_{BP}/r_{cc} \leq R \leq d_{BP}$.

Recent research has found that a two-slope propagation model is more accurate than the traditional single-slope models *ITU-R* [2009]. We find that these two models yield similar results if cell radius is large compared to the breakpoint of the two-slope model divided by the reuse factor. However, when the cell radius is short, the achievable throughput with a two-slope model is significantly lower. We observed a throughput per area that is 30 to 56% lower in the considered scenarios. This difference in throughput exists because the single-slope model uses a higher propagation exponent for devices that are closer to the transmitter. Thus, as cellular carriers reduce cell size to support growing traffic volume, the use of traditional propagation models may produce designs with inadequate capacity. Moreover, assuming that the two-slope model is correct, these results also show that the gains in capacity per area from reducing cell size get smaller when the cell radius falls below this threshold. This means that operators may find it more cost-effective at that point to meet their growing capacity needs by decreasing the frequency reuse factor or increasing spectrum holdings rather than decreasing cell size, assuming that spectrum is obtainable or that frequency reuse is not already at its minimum.

On the other hand, this work also performs a comprehensive comparison between UHF/SHF bands and millimetre wavebands considering the linear/Manhattan topology

and reuse pattern K=3, through the respective analysis of the PHY and equivalent supported throughput in 5G New Radio networks.

From this analysis, we have learned that the highest system capacity and the highest modulation and coding schemes are achievable for the shortest cell sizes at mmWaves (mainly at 28 GHz) whereas the supported throughput for long cell sizes is clearly more favourable for UHF/SHF bands. In fact, due to the behaviour arising from the two-slope propagation model (UMi LoS) applied to the 2.6 and 3.5 GHz frequency bands, the supported throughput at the mmWaves is higher than the one for the UHF/SHF bands for the shortest Rs.

Acknowledgments

This work has been partially supported and funded by CREaTION, COST CA 15104, ECOOP, UIDB/50008/2020, SFRH/BSAB/113798/2015, 3221/BMOB/16 Carnegie Mellon University Portugal Faculty Exchange Programme grant, Bolsa BID/ICI-FE/Santander Universidades-UBI/2016-17, CONQUEST (CMU/ECE/0030/2017), TeamUp5G and ORCIP.

References

V. S. Abhayawardhana, I. J. Wassell, D. Crosby, M. P. Sellars and M. G. Brown, "Comparison of empirical propagation path loss models for fixed wireless access systems," 2005 IEEE 61st Vehicular Technology Conference, Stockholm, Sweden, 2005, pp. 73-77 Vol. 1, doi: 10.1109/VETECS.2005.1543252.

IEEE 802.16m-08/004r5, IEEE 802.16m Evaluation Methodology Document, January 2009.

Guidelines for evaluation of radio interface technologies for imt-advanced, report itu-r M.2135-1 [online]. Available from: `https://www.itu.int/dms_pub/itu-r/opb/rep/R-REP-M.2135-1-2009-PDF-E.pdf`.

Sofia Sousa, Fernando J. Velez and John M. Peha, "Impact of considering the ITU-R two slope propagation model in the system capacity trade-off for LTE-A HetNets with small cells," in Proc. of 2017 XXXIInd General Assembly and Scientific Symposium of the International Union of Radio Science (URSI GASS), Montreal Quebec, Canada, vol. 2015, no. 1, 2015, pp. 189, doi: 10.1186/s13638-015-0371-9.

Emanuel Teixeira and Fernando J. Velez, "Cost/Revenue Trade-off of Small Cell Networks in the Millimetre Wavebands", in Proc. of 2018 IEEE 87th Vehicular Technology Conference: VTC2018-Spring, Porto, Portugal, 3–6 June 2018.

Guidelines for evaluation of radio transmission technologies for imt-2000, report itu-r m.1255-1. Available from: `https://www.itu.int/dms_pubrec/itu-r/rec/m/R-REC-M.1225-0-199702-I!!PDF-E.pdf` cited April of 2018.

Advanced A Practical Systems Approach to Understanding 3GPP LTE Releases 10 and 11 Radio Access Technologies, Academic Press, 2014. (isbn: "978-0-12-405162-1").

S. Rangan, T. S. Rappaport and E. Erkip, "Millimeter-Wave Cellular Wireless Networks: Potentials and Challenges", Proceedings of the IEEE, vol. 102, no. 3, pp. 366-385, March 2014, doi: 10.1109/JPROC.2014.2299397.

Fernando J. Velez, Aspects of cellular planning in Mobile Broadband Systems. Diss. Ph. D. Thesis, Instituto Superior Técnico, Lisbon, Portugal, 2000.

Fernando J. Velez et al., "Basic Limits for LTE-Advanced Radio and HetNet Optimization in the Outdoor-to-indoor Scenario", in Proc. of IEEE BlackSeaCom 2016, Varna, Bulgaria, June 2016, doi: 10.1109/BlackSeaCom.2016.7901561.

Daniel Robalo and Fernando J. Velez, "Economic trade-off in the optimization of carrier aggregation with enhanced multi-band scheduling in LTE-Advanced scenarios," EURASIP Journal on Wireless Communications and Networking, vol.

2015, no. 1, 2015, pp. 189, doi: 10.1186/s13638-015-0371-9.

3GPP, TS 36.212, V11.3.0. Technical, Specification Group Radio Access Network, Evolved Universal Terrestrial Radio Access (E-UTRA); Multiplexing and channel coding, 3GPP Std., June 2013.

3GPP, TS 36.212, V11.3.0. Technical, Specification Group Radio Access Network, Evolved Universal Terrestrial Radio Access (E-UTRA); Multiplexing and channel coding, 3GPP Std., June 2013.

Guidelines for evaluation of radio transmission technologies for imt-2000, report itu-r m.1255-1. Available from: `http://www.5gamericas.org/en/` cited April of 2018.

Bruno Cruz da Silva, Optimization of Small Cells Deployment and Frequency Assignment using Spectrum Sharing. Msc. Thesis, Universidade da Beira Interior, Covilhã, Portugal, 2018.

ITU towards "IMT for 2020 and beyond". Available from: `https://www.itu.int/en/ITU-R/study-groups/rsg5/rwp5d/imt-2020/Pages/default.aspx` cited April of 2018.

S. Min and H. L. Bertoni, "Effect of path loss model on CDMA system design for highway microcells" VTC '98. 48th IEEE Vehicular Technology Conference. Pathway to Global Wireless Revolution (Cat. No.98CH36151), Ottawa, Ontario, 1998, pp. 1009-1013 vol.2, doi: 10.1109/VETEC.1998.686392.

M. S. Mollel and M. Kisangiri, "An overview of various propagation model for mobile communication," Proceedings of the 2nd Pan African International Conference on Science, Computing and Telecommunications (PACT 2014), Arusha, Tanzânia, 2014, pp. 148-153, doi: 10.1109/SCAT.2014.7055150.

S. Ju and T. S. Rappaport, "Millimeter-Wave Extended NYUSIM Channel Model for Spatial Consistency," in Proc. of 2018 IEEE Global Communications Conference (GLOBECOM), Abu Dhabi, United Arab Emirates, 2018, pp. 1-6, doi: 10.1109/GLOCOM.2018.8647188.

E. Teixeira, F. J. Velez and J. M. Peha, "Economic Trade-off of Small Cell Networks: Comparison between the Millimetre Wavebands and UHF/SHF bands," in Proc. of 2019 IEEE 30th Annual International Symposium on Personal, Indoor and Mobile Radio Communications (PIMRC), Istanbul, Turkey, 2019, pp. 1-5, doi: 10.1109/PIMRC.2019.8904874.

T. S. Rappaport, R.W. Heath, R.C. Daniels, and J.N. Murdock, *Millimeter Wave Wireless Communications* 2015 isbn: 9780132172288, Communications Engineering and Emerging Technology Series from Ted Rappaport Series, Prentice Hall, 2015.

T. S. Rappaport, B. D. Woerner, J. H. Reed, *Wireless personal communications: The evolution of personal communications systems* 1994 isbn: 0792396766, 9780792396765, The Springer International Series in Engineering and Computer Science, Springer US, 1996.

G. R. MacCartney, Junhong Zhang, Shuai Nie and T. S. Rappaport, "Path loss models for 5G millimeter wave propagation channels in urban microcells," in Proc. of 2013 IEEE Global Communications Conference (GLOBECOM), Atlanta, GA, USA, 2013, pp. 3948-3953, doi: 10.1109/GLOCOM.2013.6831690.

D. S. Baum, J. Salo, G. Del Galdo, M. Milojevic, P. Kyösti, and J. Hansen, "An interim channel model for beyond-3G systems," in Proc. of 2005 IEEE 61st Vehicular Technology Conference Spring, Stockholm, Sweden, May 2005.

IST-WINNER D1.1.2 P. Kyösti, et al., "WINNER II Channel Models", ver 1.1, Sept. 2007. Available: `https://www.istwinner.org/WINNER2`.

A. Karttunen, J. Jarvelainen, A. Khatun and K. Haneda, "Radio Propagation Measurements and WINNER II Parameterization for a Shopping Mall at 60 GHz," in Proc. of 2015 IEEE 81st Vehicular Technology Conference (VTC Spring), Glasgow, Scotland, UK, 2015, pp. 1-5, doi: 10.1109/VTCSpring.2015.7146037.

M. K. Samimi, T. S. Rappaport and G. R. MacCartney, "Probabilistic omnidirectional path loss models for millimeter-wave outdoor communications", IEEE Wireless Communications Letters, vol. 4, no. 4, pp. 357-360, Aug. 2015.

K. Haneda et al., "5G 3GPP-Like Channel Models for Outdoor Urban Microcellular and Macrocellular Environments," in Proc. of 2016 IEEE 83rd Vehicular Technology Conference (VTC Spring), Nanjing, 2016, pp. 1-7, doi: 10.1109/VTC-Spring.2016.7503971.

"METIS Channel Model", Tech. Rep. METIS2020 Deliverable D1.4 v3, July 2015, Available: https://www.metis2020.com/wp-content/uploads/METIS.

Claude Oestges, Nicolai Czink, Philipe De Donker, Vittorio Degli-Esposti, Katsuyuki Haneda, Wout Joseph, Martine Liénard, Lingfeng Liu, José Molina-García-Pardo, Milan Narandžić, Juho, Poutanen, François Quitin and Emmeric Tanghe, "Radio Channel Modeling for 4G Networks," Chapter 10 in the book *Pervasive Mobile and Ambient Wireless Communications* (COST Action 2100), edited by Roberto Verdone and Alberto Zanella, Springer, London, UK, 2012 (ISBN 978-1-4471-2314-9), pp. 407-460.

http://www.cost2100.org/.

"New ETSI Group on Millimetre Wave Transmission starts work", Tech. Rep., [online] Available: http://www.etsi.org/news-events/news/866-2015-01-press-new-etsi-group-on-millimetre-wave-transmission-starts-work.

Available: http://www.nist.gov/ctl/wireless-networks/5gmillimeterwavechannelmodel.cfm.

"Channel modeling and characterization", Tech. Rep. MiWEBA Deliverable D5.1, June 2014, [online] Available: http://www.miweba.eu/wp-content/uploads/2014/07/MiWEBA.

mmMagic, Available: https://5g-ppp.eu/mmmagic/.

Rappaport, T. S., Sun, S., Mayzus, R., Zhao, H., Azar, Y., Wang, K., Wong, G. N., Schulz, J. K., Samimi, M., Gutierrez, F. (2013). Millimeter wave mobile communications for 5G cellular: It will work! IEEE Access, 1, 335-349. [6515173]. https://doi.org/10.1109/ACCESS.2013.2260813.

T. S. Rappaport, G. R. MacCartney, M. K. Samimi and S. Sun, "Wideband millimeter-wave propagation measurements and channel models for future wireless communication system design", IEEE Transactions on Communications, vol. 63, no. 9, pp. 3029-3056, Sept. 2015.

G. R. Maccartney, T. S. Rappaport, S. Sun and S. Deng, "Indoor Office Wideband Millimeter-Wave Propagation Measurements and Channel Models at 28 and 73 GHz for Ultra-Dense 5G Wireless Networks," in IEEE Access, vol. 3, pp. 2388-2424, 2015, doi: 10.1109/ACCESS.2015.2486778.

M. K. Samimi, T. S. Rappaport and G. R. MacCartney, "Probabilistic omnidirectional path loss models for millimeter-wave outdoor communications", IEEE Wireless Communications Letters, vol. 4, no. 4, pp. 357-360, Aug. 2015.

3GPP, "3GPP TR 21.915, "Technical specification group services and system aspects; release 15 descriptions; summary of Rel-15 work items (release15)", https://portal.3gpp.org/desktopmodules/Specifications/SpecificationDetails.aspx?specificationId=3389.

3GPP, TS 36.212, V11.3.0. Technical Specification Group Radio Access Network, Evolved Universal Terrestrial Radio Access (E-UTRA), Multiplexing and channel coding, 3GPP Std, June 2013.

3GPP, TS 38.214, Physical Layer Procedures for Data (Release 15), December 2018.

3GPP, TS 38.104 V17.0.0 (2020-12), Base Station (BS) radio transmission and reception (Release 17), December 2020.

E. Dahlman, S. Parkvall, 5G NR: The Next Generation Wireless Access Technology, Academic Press, August 2018.

S. Ahmadi, *5G NR* 2015 isbn: 9780081022672, Architecture, Technology, Implementation, and Operation of 3GPP New Radio Standards, Elsevier, 2019.

Chih-Ping Li, Jing Jiang, W. Chen, Tingfang Ji and J. Smee, "5G ultra-reliable and low-latency systems design," 2017 European Conference on Networks and Communications (EuCNC), Oulu, Finland, 2017, pp. 1-5, doi: 10.1109/EuCNC.2017.7980747.

3GPP, "5G; NR; Physical layer; General description (3GPP TS 38.201 version 15.0.0 Release 15)". Available online: `https://portal.3gpp.org/desktopmodules/Specifications/SpecificationDetails.aspx?specificationId=3211`,

Prasad, Ramjee; Velez, Fernando J.. *WiMAX Networks*. SpringerVerlag. 2010. 10.1007/978-90-481-8752-2.

Guidelines for evaluation of radio interface technologies for IMT-2020, report ITU-R m.2412-0 [online]. Available from: `https://www.itu.int/dms_pub/itu-r/opb/rep/R-REP-M.2412-0-2017-PDF-E.pdf`.

Technical feasibility of IMT in bands above 6 GHz, Report ITU-R M.2376-0 [online]. Available from: `https://www.itu.int/dms_pub/itu-r/opb/rep/R-REP-M.2376-0-2015-PDF-E.pdf`.

C. A. Fernandes, P. O. Frances and A. M. Barbosa, "Shaped coverage of elongated cells at millimetrewaves using a dielectric lens antennas," 1995 25th European Microwave Conference, Bologna, Italy, 1995, pp. 66-70, doi: 10.1109/EUMA.1995.336918.

F.J. Velez and J.M. Brázio, "A Computational-Geometry-Based Tool for the Cellular Design of Millimeterwave Mobile Communications Systems in Urban Environments," First CGC Workshop on Computational Geometry, Baltimore, USA, Oct. 1996 (http://citeseer.nj.nec.com/67742.html).